



Insulating conduction in Sn/Si(111): Possibility of a Mott insulating ground state and metallization/localization induced by carrier doping

Toru Hirahara,^{*} Taku Komorida, Yan Gu, Fumitaka Nakamura,[†] Hiroshi Idzuchi,[†] Harumo Morikawa,[‡] and Shuji Hasegawa
Department of Physics, University of Tokyo, 7-3-1 Hongo, Bunkyo-ku, Tokyo 113-0033, Japan

(Received 22 October 2009; published 11 December 2009)

The transport properties of the Si(111) $\sqrt{3} \times \sqrt{3}$ -Sn surface are investigated by micro-four-point-probe conductivity measurements. The temperature dependence of the surface-state conductivity showed an insulating behavior from room temperature down to 15 K although the surface was believed to be metallic. Furthermore, with changing the band filling by partially replacing Sn atoms with In or Na deposition, we found that the conductivity showed a metallic behavior down to 260 K and upon further cooling, the carriers became strongly localized possibly due to the dopants themselves. Our result suggests that the ground state of this surface is insulating with a very small energy gap, which is consistent with a recent theoretical study [G. Profeta and E. Tosatti, *Phys. Rev. Lett.* **98**, 086401 (2007)] predicting this surface to be a Mott insulator.

DOI: [10.1103/PhysRevB.80.235419](https://doi.org/10.1103/PhysRevB.80.235419)

PACS number(s): 73.20.-r, 68.35.-p, 73.25.+i

I. INTRODUCTION

Low-dimensional electronic systems exhibit exotic quantum phenomena, such as non-Fermi liquid behavior,¹ massless Dirac particles,² or metallic edge states of topological insulators.³ Nanostructures self-assembled on a semiconductor surface are good playgrounds to explore such quantum phenomena. The electronic structure of these systems has been studied extensively with experimental techniques such as angle-resolved photoemission spectroscopy (ARPES) or scanning tunneling microscopy/spectroscopy (STM/STS). Recently, another technique has been developed to explore the electron transport phenomena in these systems: micro-four-point probes (MFPPs).⁴ It has succeeded in detecting a temperature-dependent surface-state metal-insulator transition⁵ reported by ARPES for Si(111) 4×1 -In.⁶

From conductivity measurements, we can sometimes obtain information concerning the carrier dynamics such as localization and correlation, that are difficult to obtain just from the band dispersion.⁷⁻⁹ Taking advantage of this point, we focus on another interesting system, the Si(111) $\sqrt{3} \times \sqrt{3}$ -Sn surface, formed by 1/3 ML (1 ML=7.83 $\times 10^{14}$ atoms/cm²) of tin (Sn) atom deposition on the Si(111) surface. In contrast to the similar Si(111) $\sqrt{3} \times \sqrt{3}$ -Pb and the Ge(111) $\sqrt{3} \times \sqrt{3}$ -Sn/Pb surfaces, which undergo an order-disorder type phase transition to the 3×3 structure at low temperatures,¹⁰ this surface structure was shown to keep the $\sqrt{3} \times \sqrt{3}$ periodicity down to 6 K.¹¹ There is a debate whether the Sn atoms are vertically fluctuating [Fig. 1(a)] or static [Fig. 1(b)]. Experimental studies on the electronic structure favored the fluctuating model, showing a metallic band structure in ARPES as expected from simple electron counting with a 3×3 periodicity even at room temperature (RT).¹² Furthermore, two components in the Sn *4d* core-level spectra were found both at RT and at 70 K, which were assigned to be from the down and up positions.¹² For the idea of a static flat surface, a Mott-Hubbard insulating ground state was proposed theoretically due to the strong electron correlation effects,^{10,13} and some indication was also found experimentally, showing an energy gap opening below 70 K.¹⁴ The 3×3 periodicity of the band structure in this

model was explained as due to the short-range antiferromagnetic spin ordering. Therefore, it is highly desirable to perform other experimental works to determine which of the two models is really correct. Moreover it is well-known that high-temperature cuprate superconductors are realized by doping carriers into a Mott insulator.¹⁵ If carriers in a surface Mott insulator can be doped, it would be a nice example to examine the presence of surface-state superconductivity.¹³

In the present work, we have performed MFPP conductivity measurements on this Si(111) $\sqrt{3} \times \sqrt{3}$ -Sn surface to investigate the intriguing issues discussed above. We found that throughout the measured temperature range (15–300 K), the surface-state conductivity decreased by decreasing the temperature, an insulating behavior. The results are consistent with the report of Ref. 14, insisting that the surface behaves as a “bad metal” from 300 K down to 70 K and an energy gap opens up below 70 K and indeed suggests that correlation effects are important on this surface.¹³ Furthermore by carrier doping to the surface by replacing Sn with In atoms [Fig. 1(c)] or additional Na deposition [Fig. 1(d)], we found that the conductivity shows a metallic behavior from 300 to 260 K. At lower temperatures, however, the carriers were strongly localized possibly due to the defects induced by the dopants, which prevented the examination of surface-state superconductivity.

II. EXPERIMENTAL

The conductivity measurements were performed using a custom-made ultrahigh vacuum chamber for *in situ* MFPP measurement equipped with a reflection-high-energy electron diffraction (RHEED) system.⁴ The probe spacing was 20 μm . Four probe conductivity measurements can be performed without any perceptible damages on the surface.¹⁶ The temperature-dependent measurements were performed while the sample was cooled down from room temperature. Additionally, ARPES experiments were performed with a commercial hemispherical photoelectron spectrometer (VG ADES-400) using unpolarized He I α (21.2 eV) radiation at room temperature. The Fermi level position (E_F) was deter-

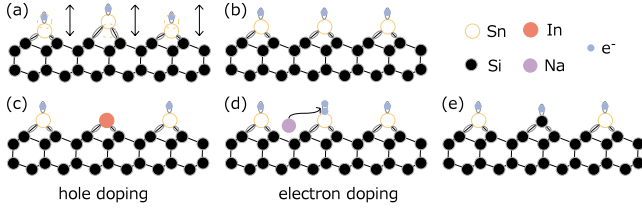


FIG. 1. (Color online) Schematic drawings (side view) of the fluctuating (a) and static (b) models of Si(111) $\sqrt{3}\times\sqrt{3}$ -Sn, the In-replaced (c) and Na-deposited (d) surfaces to manipulate the band filling, and the mosaic $\sqrt{3}\times\sqrt{3}$ surface (e).

mined by measuring the metallic Fermi edge of a Ta foil fixed on the sample holder. STM measurements were performed with a commercial LT-STM (UNISOKU USM501 type) at 65 K. A chemically etched W tip was used. An *n*-type (1–10 Ω cm at 300 K) Si(111) wafer was used as the substrate. The Si(111)- 7×7 clean surface was prepared by direct current heating up to 1500 K for a few seconds. Sn and In were evaporated from outgassed alumina-coated W baskets onto Si(111)- 7×7 at RT followed by annealing up to 800 K for 30 s. Sodium deposition was performed using a thoroughly outgassed SAES getter source. The deposition rate of each material was calibrated by the formation of $\sqrt{3}\times\sqrt{3}$ and $2\sqrt{3}\times 2\sqrt{3}$ phases for Sn, $\sqrt{3}\times\sqrt{3}$, $\sqrt{31}\times\sqrt{31}$, and 4×1 phases for In, and $\delta 7\times 7$ and 3×1 phases for Na.¹⁷

III. RESULTS AND DISCUSSIONS

A. Pristine surface

Figure 2(a) shows the measured resistance as a function of the temperature (15–300 K) for the pristine Si(111) $\sqrt{3}\times\sqrt{3}$ -Sn surface. The red empty and black filled circles show the data for two separate measurements. We find that the resistance increases as the temperature is lowered in the whole temperature range. Therefore, it can be said that an insulating behavior is seen from RT all the way down to 15 K [inset of Fig. 2(a)]. In the MFPP method, the bulk contribution can be neglected^{5,7} and the measured resistance (R) can be divided into the sum of the surface-state conductivity (σ_{ss}) and that of the space-charge layer (σ_{sc}) just beneath the surface layer as $\frac{\ln 2}{\pi R} = \sigma_{ss} + \sigma_{sc}$. The space-charge layer contribution can be calculated if the band bending is known.^{4,7} Since the surface Fermi level position for the Si(111) $\sqrt{3}\times\sqrt{3}$ -Sn surface is $E_F - E_{VBM} = 0.50$ eV as obtained by Si 2*p* core-level photoemission,¹⁸ the space-charge layer is a depletion type and σ_{sc} is negligible compared to the measured value of ~ 25 $\mu\text{S}/\square$ at RT. As the space-charge layer contribution, furthermore, decreases quickly upon cooling,^{5,7} the measured resistance can be interpreted as the surface-state contribution alone, $\frac{\ln 2}{\pi R} = \sigma_{ss}$ in the whole temperature range.

Therefore, it can be said that σ_{ss} of Si(111) $\sqrt{3}\times\sqrt{3}$ -Sn shows an insulating behavior. However, as written above, the surface has a metallic electronic structure at RT as well as at lower temperatures^{12,18,19} as revealed by ARPES. On the other hand, the conductivity value at RT is smaller than the Ioffe-Regel criterion of 39 $\mu\text{S}/\square$ in two dimensions for me-

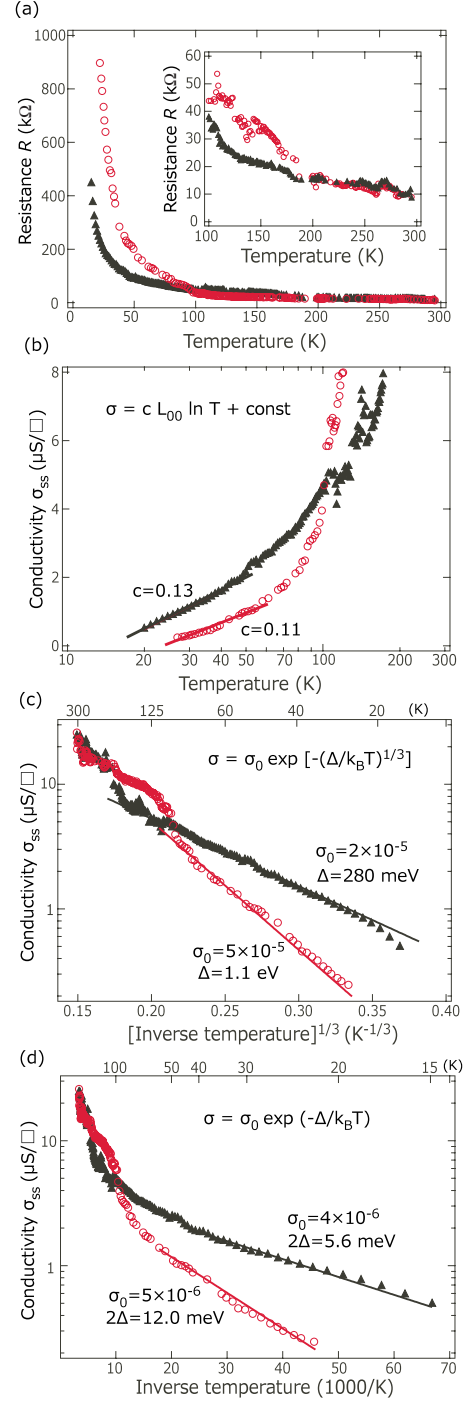


FIG. 2. (Color online) (a) The temperature dependence of the measured resistance of the pristine Si(111) $\sqrt{3}\times\sqrt{3}$ -Sn surface (red empty and black filled circles for two separate measurements). The inset shows the enlarged view of the data points for 100–300 K. (b) The obtained surface-state conductivity ($\sigma_{ss} = \ln 2 / \pi R$) plotted as a function of the logarithm of temperature for the two different data sets of the pristine Si(111) $\sqrt{3}\times\sqrt{3}$ -Sn surface shown in (a). The solid lines show a fitting to Eq. (1). (c) The surface-state conductivity (σ_{ss}) plotted as a function of the [inverse of temperature]^{1/3} for the data sets shown in (a). The solid lines show a fitting to Eq. (2). (d) The surface-state conductivity (σ_{ss}) plotted as a function of the inverse of temperature for the data sets shown in (a). The solid lines show a fitting to Eq. (4).

tallic conduction.⁸ This suggests that the surface is not a simple metal.

Insulating behavior in the conductivity for a metallic system has been found in other materials with disorder, such as ion-radiated SrRuO₃.²⁰ They show a weak localization behavior which can be expressed as (two-dimensional case),²¹

$$\sigma = cL_{00} \ln T + \text{const}, \quad (1)$$

where c and const are fitting parameters, and $L_{00} = 12.3$ (μS) (quantum conductance divided by 2π). The value of c ($\approx 1 \sim 2$) is related to the temperature dependence of the phase relaxation time of carriers. We have therefore first assumed that due to the inevitable defects formed at the surface, the carriers of the Si(111) $\sqrt{3} \times \sqrt{3}$ -Sn surface are weakly localized and show insulating behavior already from room temperature. Figure 2(b) shows the surface-state conductivity (σ_{ss}) plotted as a function of the logarithm of temperature for the two measurements, respectively. The linear fitting is valid only for a very small temperature range (below 60 K) and the obtained values of c are 0.13 ± 0.01 and 0.11 ± 0.01 , respectively, which are an order or magnitude smaller than the theoretical value of $c \approx 1 \sim 2$. Although this may be suggesting that some new theory is needed to account for the phase relaxation of this surface, we conclude that it is unlikely that weak localization is governing the conduction mechanism in the present case.

Let us now consider the case of a stronger localization effect, such as variable-range hopping (VRH).² Recently, H-adsorbed graphene formed on SiC was found to exhibit a VRH behavior although the band structure was still metallic.²² The temperature dependence of the conductivity can be expressed as

$$\sigma = \sigma_0 \exp[-(\Delta/k_B T)^{1/3}], \quad (2)$$

where σ_0 is the pre factor and Δ is the activation energy. Figure 2(c) shows the data of Fig. 2(a) fitted to Eq. (2) below 150 K. The obtained values of activation energy are 280 ± 10 and 1100 ± 50 meV for the two different data sets, respectively. The localization length ξ can be obtained as

$$\xi = \sqrt{\frac{3^3}{\pi} \frac{1}{\Delta D^{2D}}}, \quad (3)$$

where D^{2D} is the two-dimensional density of state at the Fermi level. Using the values reported in Ref. 18, ξ is calculated as 20–40 Å. Since tiny amounts of defect formation are unavoidable at the surface, it can be plausible that some localized state will be formed around these defects and the conductivity will obey the VRH behavior.

So what are other possibilities left? Let us recall the recent publication by Modesti *et al.*¹⁴ Through detailed STS measurements, they have found that although the surface is metallic at RT, the density of state (DOS) at the Fermi level (E_F) decreases gradually by lowering the temperature (bad metal), and finally a clear gap opens up at E_F around 70 K.¹⁴ In view of their finding, our data can be interpreted as follows. From the Boltzmann equation, the electrical conductivity for an isotropic two-dimensional metallic system can be expressed as $\sigma = \frac{e^2}{2} l v_F D^{2D}$, where l is the mean-free path, v_F

is the Fermi velocity, and D^{2D} is the DOS at E_F .²³ The ARPES studies suggest that Si(111) $\sqrt{3} \times \sqrt{3}$ -Sn has a nearly free electron-like metallic band dispersion,^{18,19} justifying the use of this equation. In usual metallic systems, l becomes larger upon cooling due to the suppressed phonon scattering without basically any change in v_F or D^{2D} , resulting in the increase of σ . However, in the present case, we think that although l does become larger by lowering the temperature, D^{2D} decreases as revealed by STS, which likely determines the insulating behavior of the conductivity.

Below 70 K, it is said that the surface has a band gap and becomes an insulator.¹⁴ Then the conductivity should be described by a simple thermal activation type,

$$\sigma = \sigma_0 \exp(-\Delta/k_B T), \quad (4)$$

where Δ is the activation energy. The energy gap near E_F can be obtained as 2Δ . Figure 2(d) shows σ_{ss} plotted as a function of the inverse temperature for the two measurements, respectively. We indeed see that the slopes of the curves in Fig. 2(d) change at ~ 80 K, confirming that the conduction mechanism changes around this temperature. The obtained energy gaps are 12.0 ± 0.2 and 5.6 ± 0.2 meV for the two curves.²⁴ This is compatible with the value reported in Ref. 14, showing an upper limit of 40 meV, although somewhat smaller²⁵ and does not correspond to any other energies in the band structure. The resolution of the STS measurements in Ref. 14 may not have been enough to determine such a small gap. The reports of previous ARPES measurements that the band structure does not change at low temperature^{12,19} may also be attributed to the insufficient instrumental resolution, surface photovoltage effects or the different temperatures (70 K in Ref. 12 and 130 K in Ref. 19). Furthermore, Ref. 14 shows that the size of the energy gap is site dependent. The value we have obtained may be an average of such site-dependent gaps and may be influenced by the sample preparation methods.

Our finding of a possibility of an insulating ground state is also in agreement with the recent theoretical proposal of the Si(111) $\sqrt{3} \times \sqrt{3}$ -Sn surface to have an antiferromagnetic Mott-Hubbard ground state,¹³ although the knowledge of spin configuration of the Sn sites remains to be clarified. Although the Peierls transition can also induce insulating ground states at low temperature,⁵ the absence of a good nesting vector as well as the fact that there is no change in the surface periodicity insists that this is unlikely,¹⁸ and we think that the Mott transition scenario is the most likely for this surface. Recently, it was reported that the similar Sn/Ge surface has a metallic ground state.^{26,27} In Ref. 13, the authors have pointed out that there is only a slight energy difference between the metallic and Mott insulating phases, and we believe that the difference of the substrate (Si or Ge) leads to a subtle change in the energy balance and therefore to different ground states. The gap size in the present case is much smaller than that reported in other Mott insulating phases on semiconductor surfaces.^{28,29} This is also probably due to the very small energy difference between the Mott insulating phase and the metallic phase.¹³

To conclude this section, we have found an insulating conduction behavior for Si(111) $\sqrt{3} \times \sqrt{3}$ -Sn. This can be ei-

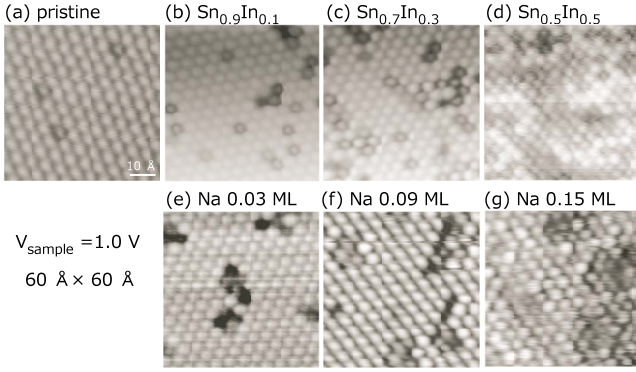


FIG. 3. (Color online) STM images ($60 \text{ \AA} \times 60 \text{ \AA}$, $V_{\text{sample}} = 1 \text{ V}$) of the $\text{Si}(111)\sqrt{3} \times \sqrt{3}-(\text{Sn}_{1-x}\text{In}_x)$ surfaces (a)–(d), and Na deposited $\text{Si}(111)\sqrt{3} \times \sqrt{3}-\text{Sn}$ surfaces (e)–(g), respectively.

ther interpreted as a variable-range hopping due to the inevitable defects at the surface, or to an energy gap opening due to a transition to a Mott insulating ground state upon cooling.

B. Carrier-doped surfaces

1. Geometric and electronic structures of the doped surfaces

Now that we have obtained some evidence that $\text{Si}(111)\sqrt{3} \times \sqrt{3}-\text{Sn}$ has an insulating ground state, we have tried to change the band filling. If the surface is a Mott insulator, it can be expected that by carrier doping, metallic conductivity or even superconductivity may be realized. To reduce the carrier density (hole doping), we have replaced some Sn with In atoms, which is trivalent compared to the tetravalency of Sn and also sits on T_4 sites on the $\text{Si}(111)$ surface [Fig. 1(c)]. As shown in the STM images of Figs. 3(a)–3(d), the number of defects, which appear dark has increased compared to the pristine surface, and these defects should correspond to the replaced In atoms. We observed no phase separation; i.e., we could not observe any regions that are $\sqrt{3} \times \sqrt{3}-\text{Sn}$ and other regions that are $\sqrt{3} \times \sqrt{3}-\text{In}$. On the other hand, to increase the carriers (electron doping), we have deposited alkali metals, namely Na atoms on the pristine $\text{Si}(111)\sqrt{3} \times \sqrt{3}-\text{Sn}$ surface [Fig. 1(d)]. The STM images of such Na-deposited surface is shown in Figs. 3(e)–3(g). We can also find the area of defects, which appear dark is increasing upon Na deposition. For high defect coverage [Figs. 3(d) and 3(g)] there are some regions where the defect seems to appear brighter than the Sn atoms on the pristine surface. The details of the STM observation will be reported elsewhere.³⁰ The surface periodicity observed by RHEED in both of the above cases showed the $\sqrt{3} \times \sqrt{3}$ patterns, which were a bit weaker than that of the pristine surface.

To confirm if the band filling can actually be manipulated by the above two methods, we have also performed ARPES measurements. Figure 4(a) shows the schematic drawing of the band dispersion of $\text{Si}(111)\sqrt{3} \times \sqrt{3}-\text{Sn}$ adapted from Ref. 19. As mentioned in the introduction, the band structure follows the 3×3 periodicity and the bottom of the half-filled metallic band is located at the $\bar{K}_{\sqrt{3} \times \sqrt{3}}(\bar{\Gamma}_{3 \times 3})$ point. We have measured the spectra at this point for the pristine,

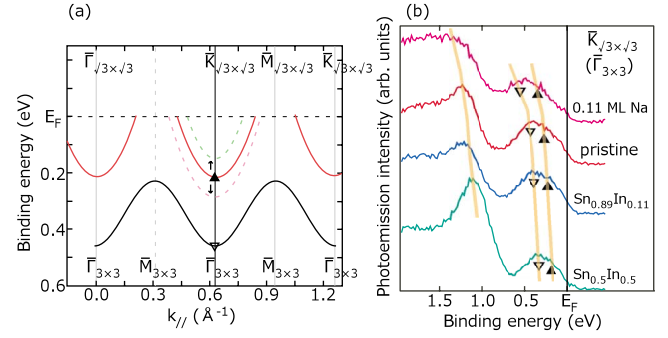


FIG. 4. (Color online) (a) Schematic drawing of the band structure near the Fermi level for the $\text{Si}(111)\sqrt{3} \times \sqrt{3}-\text{Sn}$ (solid lines) taken from the data of Ref. 19. The dotted lines show the dispersion of the metallic band after carrier doping. (b) The photoemission spectra at the $\bar{K}_{\sqrt{3} \times \sqrt{3}}(\bar{\Gamma}_{3 \times 3})$ point for the pristine, In-replaced and Na-adsorbed $\text{Si}(111)\sqrt{3} \times \sqrt{3}-\text{Sn}$ surfaces. The empty and filled triangles show the peak positions which is clearly shifted due to the manipulation of the carrier filling.

$\text{Si}(111)\sqrt{3} \times \sqrt{3}-(\text{Sn}_{1-x}\text{In}_x)$ ($x=0.1, 0.5$), and 0.11 ML Na deposited $\text{Si}(111)\sqrt{3} \times \sqrt{3}-\text{Sn}$ surfaces, which are shown in Fig. 4(b). The broad peak near the Fermi level actually consists of two peaks, as indicated by the filled (open) triangles at lower (higher) binding energy.¹⁹ There is also another one at $\sim 1 \text{ eV}$. For the In replaced surfaces, the peak position shifts closer to E_F , where as for the Na adsorbed surface, the peaks shift to higher binding energy than that of the pristine surface. This indeed reveals that the bands shift rigidly by the methods we have discussed and it is possible to change the band filling of the metallic surface state, which is shown by the dotted lines in Fig. 4(a).

2. Temperature dependence of the surface-state conductivity for the carrier-doped surfaces

Next, we have measured the temperature dependence of the surface-state conductivity for the $\text{Si}(111)\sqrt{3} \times \sqrt{3}-(\text{Sn}_{0.9}\text{In}_{0.1})$. From a simple estimation, this accounts to 10% reduction of the band filling. Furthermore, we have measured the 0.03 ML Na-deposited $\text{Si}(111)\sqrt{3} \times \sqrt{3}-\text{Sn}$ surface. Assuming that Na will donate one electron per atom, this accounts to 10% increase of the band filling.³¹

Figure 5(a) shows the measured resistance as a function of the temperature (15–300 K) for the pristine $\text{Si}(111)\sqrt{3} \times \sqrt{3}-\text{Sn}$ surface, the surface in which 10 % of Sn atoms were replaced with In, the surface with 0.03 ML of Na adsorption, and the mosaic $\sqrt{3} \times \sqrt{3}$ phase, which is formed by 1/6 ML of Sn deposition on $\text{Si}(111)-7 \times 7$.³² As can be obviously seen, all the structures show an insulating behavior (the resistance increases by decreasing the temperature) at low temperature.

Now let us look into the details. The carrier doped surfaces have higher resistance than the pristine surface below 200 K and we were unable to continue the measurement at lower temperatures because of the difficulty to obtain linear current-voltage curves in the four-point-probe resistance measurement. Figure 5(b) shows the magnified plots of Fig. 5(a) from 240 to 300 K. The solid lines are the guide to the

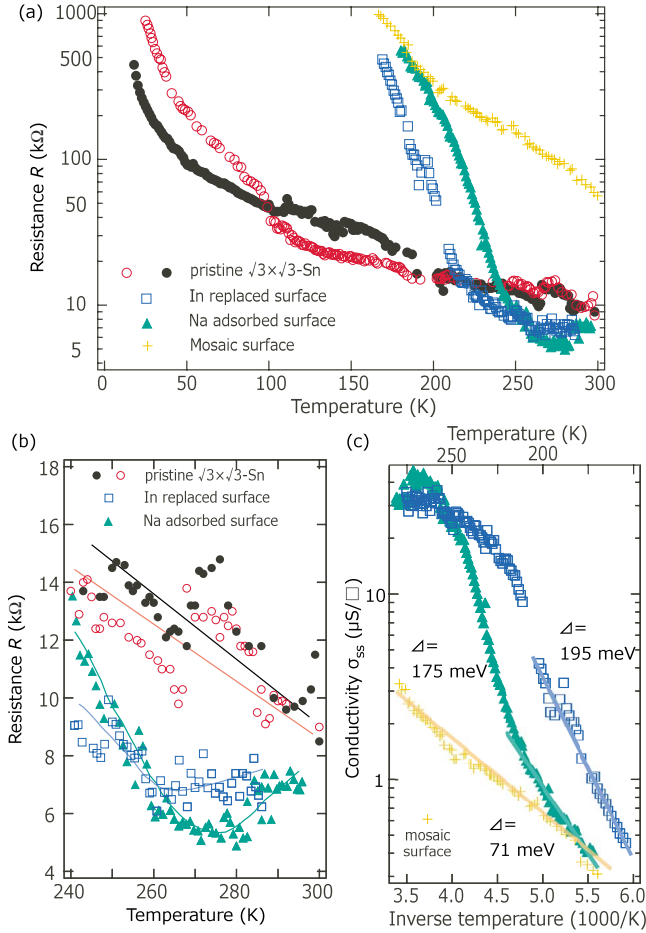


FIG. 5. (Color online) (a) The temperature dependence of the measured resistance of the pristine Si(111) $\sqrt{3}\times\sqrt{3}$ -Sn surface (red empty and black filled circles for two separate measurements) and those of the In-replaced (blue empty squares), Na-adsorbed (green filled triangles) and the mosaic (orange crosses) surfaces. (b) The magnified plots of (a) from 240 to 300 K. (c) The obtained surface-state conductivity ($\sigma_{ss}=\ln 2/\pi R$) plotted as a function of the inverse temperature for the In-replaced and Na-adsorbed Si(111) $\sqrt{3}\times\sqrt{3}$ -Sn surface shown in (a). The solid lines show a fitting to Eq. (4).

eye. For the pristine Si(111) $\sqrt{3}\times\sqrt{3}$ -Sn, the resistance rises monotonically with decreasing temperature as has been discussed above. However, for the carrier doped surfaces, we find that first the resistance shows a metallic behavior and then starts to increase at 260–270 K, a metal-insulator transition. We believe that this change to a metallic conduction at higher temperatures also supports that the Si(111) $\sqrt{3}\times\sqrt{3}$ -Sn surface is a Mott insulator,¹³ i.e., due to the reduced electron-correlation effects by the manipulation of the band filling, the surface becomes a “good metal” from a “bad metal.” For the Na-adsorbed surface, it can also be said that the Fermi level has gone above the mobility edge and results in the metallic conduction in the VRH scenario. However, such an explanation is not possible for the Sn-replaced surface. While it is difficult to conclude clearly, we believe that the elucidation based on the Mott insulating ground state is more plausible than the VRH scenario taking into account the similarity of the electron and hole doped cases.

The transition to an insulating behavior below about 260 K can be understood as follows. Because we have deposited Na or replaced Sn with In, they not only change the band filling but also act as scatterers and likely induce carrier localization, as shown in the STM images of Fig. 3. Carrier scattering at a point defect in metal crystal is generally elastic and only contributes to the residual resistance. However, at the surface, it is known that such defects can induce (strong) localization due to the weakened screening effects because of the reduced dimensionality, as has been reported for other metallic surfaces.^{7,9} To identify the transport mechanism, first we have tried to fit the data of Fig. 5(a) with the weak localization-type function, Eq. (1). However, a reasonable fitting could not be obtained and we deny the possibility of weak localization effect. Then, the VRH should be considered again [Eq. (2)]. We can actually find a reasonable fitting and the obtained activation energies are $\Delta\sim 3\text{--}5$ eV. However, for such a large activation energy, the criteria for a VRH to occur [$\frac{1}{3}(\frac{\Delta}{k_B T})^{1/3}>1$] is already fulfilled at room temperature, in contradiction to our finding of a metallic conduction near room temperature. Therefore the VRH mechanism can be excluded.

Next we have tried fitting with the thermal activation type Eq. (4). The results are shown in Fig. 5(c) and the data below 220 K were well-fitted. The obtained activation energies are 195 ± 10 and 175 ± 10 meV for the In-replaced and Na-adsorbed surfaces, respectively. What does this activation energy mean? There is no energy in the electronic band structure that corresponds to this value. One possibility may be the ionization energy of the donor/acceptor level of Na/In given by $E\sim\frac{13.6}{\epsilon^2}m^*$ eV, which can be found in solid state text books related to doping of semiconductors.³³ Using the values of $\epsilon\sim 6.4$ which is the mean value of Si and the vacuum and $m^*=0.57$,¹⁸ E is calculated as 227 meV. Even though the Si(111) $\sqrt{3}\times\sqrt{3}$ -Sn surface recovers its metallicity upon doping, the dopants induce strong scattering potentials which cannot be fully screened by the surface-state carriers⁷ and likely induce strong localization. Such localization by disorder potentials has been observed also in GaAs-AlGaAs heterostructures with low carrier density.³⁴ However, such a strong potential with large energy scales should also prohibit the metallicity completely meaning that a metallic conduction should not occur even near room temperature, which is in contradiction to our observation. The origin of this activation energy remains to be clarified in future studies.

For a comparison, we have also measured the mosaic $\sqrt{3}\times\sqrt{3}$ phase to explore the difference of the “charged” and “charge-neutral” impurities. This is because the mosaic surface is a structure in which half of the Sn atoms are replaced by group IV Si atoms.³² Therefore there is no change in the band filling as reported in Ref. 19 and the silicon atoms only act as scatterers [Fig. 1(e)]. As shown in Fig. 5(a), this surface has a much higher resistance compared to the pristine, Na-doped and In-replaced surfaces at RT. It shows a semi-conducting behavior upon cooling and the temperature dependence can be fitted with Eq. (4), which gives an activation energy of 71 ± 9 meV [Fig. 5(c)]. The defect density for the mosaic phase is much higher than the Na-doped or In-replaced surfaces. Nevertheless the activation energy is much

smaller. Although the meaning of this activation energy is not clear, this shows that charged impurities have much higher effect on the electron transport at the surface at low temperatures.

Let us now compare the present case with the situation in high temperature superconducting cuprates. Figure 5(b) clearly shows that we have actually succeeded in metallization by carrier doping. However at low temperatures, the dopants act as defects and induce strong carrier localization. The situation is different in cuprates which are quasi-2D layered materials. Dopants are usually located in the blocking layers that are spatially separated from the CuO₂ plane, the carrier conduction plane. So the carriers are not so much influenced by the dopants in cuprates. Because surfaces are only few atomic layers thick, the dopants at the same time act as strong scatterers for the surface-state carriers and it seems that their influence on the transport properties cannot be avoided, making it difficult to maintain the metallic conduction at low temperatures.

IV. CONCLUSIONS

In conclusion, from MFPP surface conductivity measurements the Si(111) $\sqrt{3} \times \sqrt{3}$ -Sn showed an insulating behavior. Furthermore, by carrier doping we succeeded in obtaining metallic conduction but have found that the dopants at the same time act as defects and induce strong carrier localization at low temperatures. This suggests that the ground state of this surface is (Mott) insulating with a very small energy gap below 80 K, which is in accordance with recent STS studies¹⁴ and *ab initio* calculations,¹³ although the surface was believed to be metallic down to 70 K.^{12,19}

ACKNOWLEDGMENTS

We acknowledge S. Yamazaki for his valuable comments. This work has been supported by Grants-In-Aid and A3 Foresight Program from Japan Society for the Promotion of Science.

*hirahara@surface.phys.s.u-tokyo.ac.jp

[†]Present address: Institute for Solid State Physics, University of Tokyo, Kashiwa 277-8581, Japan.

[‡]Present address: Institute of Physics and Applied Physics, Yonsei University, 134 Shinchon, Seoul 120-749, Korea.

¹J. M. Luttinger, *J. Math. Phys.* **4**, 1154 (1963).

²A. K. Geim and K. S. Novoselov, *Nature Mater.* **6**, 183 (2007).

³D. Hsieh, D. Qian, L. Wray, Y. Xia, Y. S. Hor, R. J. Cava, and M. Z. Hasan, *Nature (London)* **452**, 970 (2008).

⁴T. Tanikawa, I. Matsuda, R. Hobar, and S. Hasegawa, *e-J. Surf. Sci. Nanotechnol.* **1**, 50 (2003).

⁵T. Tanikawa, I. Matsuda, T. Kanagawa, and S. Hasegawa, *Phys. Rev. Lett.* **93**, 016801 (2004).

⁶H. W. Yeom, S. Takeda, E. Rotenberg, I. Matsuda, K. Horikoshi, J. Schaefer, C. M. Lee, S. D. Kevan, T. Ohta, T. Nagao, and S. Hasegawa, *Phys. Rev. Lett.* **82**, 4898 (1999).

⁷I. Matsuda, C. Liu, T. Hirahara, M. Ueno, T. Tanikawa, T. Kanagawa, R. Hobar, S. Yamazaki, S. Hasegawa, and K. Kobayashi, *Phys. Rev. Lett.* **99**, 146805 (2007).

⁸M. D'angelo, K. Takase, N. Miyata, T. Hirahara, S. Hasegawa, A. Nishide, M. Ogawa, and I. Matsuda, *Phys. Rev. B* **79**, 035318 (2009).

⁹C. Liu, I. Matsuda, S. Yoshimoto, T. Kanagawa, and S. Hasegawa, *Phys. Rev. B* **78**, 035326 (2008).

¹⁰J. Ortega, R. Pérez, and F. Flores, *J. Phys.: Condens. Matter* **14**, 5979 (2002).

¹¹H. Morikawa, I. Matsuda, and S. Hasegawa, *Phys. Rev. B* **65**, 201308(R) (2002).

¹²R. I. G. Uhrberg, H. M. Zhang, T. Balasubramanian, S. T. Jemander, N. Lin, and G. V. Hansson, *Phys. Rev. B* **62**, 8082 (2000).

¹³G. Profeta and E. Tosatti, *Phys. Rev. Lett.* **98**, 086401 (2007).

¹⁴S. Modesti, L. Petaccia, G. Ceballos, I. Vobornik, G. Panaccione, G. Rossi, L. Ottaviano, R. Larciprete, S. Lizzit, and A. Goldoni, *Phys. Rev. Lett.* **98**, 126401 (2007).

¹⁵M. Imada, A. Fujimori, and Y. Tokura, *Rev. Mod. Phys.* **70**,

1039 (1998).

¹⁶I. Shiraki, T. Nagao, S. Hasegawa, C. L. Petersen, P. Bøggild, T. M. Hansen, and F. Grey, *Surf. Rev. Lett.* **7**, 533 (2000).

¹⁷V. G. Lifshits, A. A. Saranin, and A. V. Zotov, *Surface Phases on Silicon* (Wiley, New York, 1994).

¹⁸H. Morikawa, Ph.D. thesis, University of Tokyo, 2005.

¹⁹J. Lobo, A. Tejada, A. Mugarza, and E. G. Michel, *Phys. Rev. B* **68**, 235332 (2003).

²⁰M. A. López de la Torre, Z. Sefrioui, D. Arias, M. Varela, J. E. Villegas, C. Ballesteros, C. León, and J. Santamaria, *Phys. Rev. B* **63**, 052403 (2001).

²¹N. F. Mott and E. A. Davis, *Electronic Processes in Non-crystalline Materials*, 2nd ed. (Oxford University Press, Oxford, 1979).

²²A. Bostwick, J. L. McChesney, K. V. Emtsev, T. Seyller, K. Horn, S. D. Kevan, and E. Rotenberg, *Phys. Rev. Lett.* **103**, 056404 (2009).

²³I. Matsuda, T. Hirahara, M. Konishi, C. Liu, H. Morikawa, M. D'angelo, S. Hasegawa, T. Okuda, and T. Kinoshita, *Phys. Rev. B* **71**, 235315 (2005).

²⁴The large difference in the activation energies of Figs. 2(c) and 2(d) are possibly due to the difference found in the pre factor σ_0 ; σ_0 in Fig. 2(c) is an order of magnitude larger than those found in Fig. 2(d).

²⁵The difference between the gap size determined by electrical and optical conductivity measurements (the real band gap) has also been pointed out for bulk Mott insulators. For example, see T. Katsufuji, Y. Okimoto, and Y. Tokura, *Phys. Rev. Lett.* **75**, 3497 (1995).

²⁶H. Morikawa, S. Jeong, and H. W. Yeom, *Phys. Rev. B* **78**, 245307 (2008).

²⁷S. Colonna, F. Ronci, A. Cricenti, and G. Le Lay, *Phys. Rev. Lett.* **101**, 186102 (2008).

²⁸H. H. Weitering, X. Shi, P. D. Johnson, J. Chen, N. J. DiNardo, and K. Kempa, *Phys. Rev. Lett.* **78**, 1331 (1997).

- ²⁹V. Ramachandran and R. M. Feenstra, Phys. Rev. Lett. **82**, 1000 (1999).
- ³⁰T. Komorida, T. Hirahara, and S. Hasegawa (unpublished).
- ³¹We also note that position of the bulk band peak measured at normal emission in the ARPES measurements showed little change in energy position when carriers were doped on the Si(111) $\sqrt{3} \times \sqrt{3}$ -Sn phase. This means that the space-charge layer is still a depletion layer and its conductivity can also be neglected for the carrier-doped surfaces, similar to the case of the pristine surface.
- ³²H. M. Zhang, S. T. Jemander, N. Lin, G. V. Hansson, and R. I. G. Uhrberg, Surf. Sci. **531**, 21 (2003).
- ³³C. Kittel, *Introduction to Solid State Physics*, 7th ed. (Wiley, New York, 1996).
- ³⁴E. Ribeiro, R. D. Jäggi, T. Heinzl, K. Ensslin, G. Medeiros-Ribeiro, and P. M. Petroff, Phys. Rev. Lett. **82**, 996 (1999).